International Journal Of Engineering Research And Development
e- ISSN: 2278-067X, p-ISSN: 2278-800X, www.ijerd.com
Volume 15, Issue 3 (March 2019), PP.59-68

Reproducing Photonic Radio-Frequency Memory Based on Multicore Fibers

Mikhail E. Belkin,[1,] Tatiana N. Bakhvalova,[1] Igor V. Gladyshev,[1] Dmitry A. Klushnik,[1] Olga N. Egorova[2] and Sergei L. Semenov [2]

1STC "Integrated microwave photonics", Russian Technological University MIREA, Moscow, Russian Federation

2Fiber Optics Research Center of the Russian Academy of Sciences (FORC RAS), Moscow, Russian Federation

Corresponding Author: Mikhail E. Belkin

ABSTRACT: *A novel photonic radio-frequency memory design based on microwave photonics and multicore fiber techniques is developed and investigated. The results of the prototype examination as compared to the known versions Photonic radio-frequency memory showed that the adopted design concept allowed to ensure a sufficiently deep memorization of the input radio-frequency signal, to increase the number of reproduced delay gradations, and to successfully process all the radar's radio frequency pulse width, which extends from several hundred of nanoseconds to tens of microseconds, in a multi-octave RF operating range.*

Date of Submission: 20-10-2019 Date of acceptance: 03-11-2019

I. INTRODUCTION

Last two decades are characterized by onrushing microwave photonics (MWP) techniques in the design of next-generation radio-electronic systems on commercial and military platforms. The key areas of the MWP investigator's endeavors include wireless communication, radar, and electronic warfare equipment (Seeds and Williams, 2006; Capmany and Novak, 2007; Yao, 2009). To date the preponderance over traditional electronic approach has been successfully demonstrated for the particular basic processing procedures of a microwave-band network: microwave signal oscillation, intermediate processing (modulation, up- or down-conversion, filtering, etc.), and time retarding in optical region (see Urick et al., 2015 and references cited therein).

The details of year-to-year progress in the R&Ds referred to the above-mention devices during the last 20 years are reflected in the proceedings of International Topical Meeting on Microwave Photonics (http://ieeexplore.ieee.org/xpl/conhome.jsp?punumber=1000458).

Regarding the last processing procedure, there are many worldwide suppliers manufacturing fiber-optic delay lines (FODL).The key advantage of this approach is in the direct processing of RF signals utilizing low propagation loss, vast instantaneous bandwidth, and insensitivity to electromagnetic interference of optical fiber. To date, two modifications of FODL are available: fixed-length one and more versatile FODL with adjustable delay (Diehl et al., 2015) including a series of delay and switch elements in a binary arrangement to provide a pure replica of multiple possible delays. An example of a state-of-the-art binary fiber optic delay line (BiFODL) is described in References (Urick, 2015; Diehlet al., 2015). Its block diagram includes a single high-power laser emitter, Mach-Zehnder modulator (MZM), long binary delay chain where optical switches are used to switch in or out delay segments, and at least seven optical amplifiers to compensate losses in passive network. However, BiFODL has a general lack in comparison with electronic digital radio-frequency memory (DRFM): it cannot provide multiple replicas of a single input radio frequency (RF) signal (or memory), which is a concern for a number of very important radar test and evaluation (Olivier K. and Gouws M. 2013) as well as of anti-radar Electronic countermeasure (ECM) techniques (Kwak,2009).

A prospective way to create a device for short-term storing RF signals is so-called photonic RF memory (PRFM) based on recirculating delay line (RDL) structure. This technique has been known for near thirty years and today two key approaches for its realization are under exploration using optoelectronic or all-optical concept. An example of the first one (Koffman et al., 1988) based on a hybrid loop consists of low-noise RF amplifier with RF switch element on its input, and MWP feedback circuit including optical transmitting unit for electrical-to-optical (E/O) conversion, 280-m multimode fiber for the delay procedure, as well as optical receiving unit for optical-to-electrical (O/E) conversion, on its output. Although as many as 39 circulations were experimentally demonstrated in the operating frequency range of 2–6 GHz, its storage time and instantaneous bandwidth (IBW) are strongly limited by the rapid accumulation of noise and numerous E/O and O/E conversions degrading the RF signal during each circulation in the loop. These shortcomings were eliminated in the second conceptual realization (Nguyen et al., 2014) by introducing an optical amplifier and a

frequency shift unit inside the loop and utilizing input and output optical switches to open it only at the moments when a delayed RF pulse passes. Thereby it was supported more than 100 circulations while the signal-to-noise ratio (SNR) degradation was no more than 7 dB.

Nevertheless, both known schemes do not meet the modern requirements of practical radars and ECM means, since they cannot successfully process all the radar's RF pulse width, which extends from several hundred of nanoseconds to tens of microseconds, in a multi-octave RF operating range (Baldwinson and Antipov, 2008). Therefore, a more complex multi-stage PRFM circuitry is needed, which at the same time must meet the stringent requirements of military equipment in terms of cost-efficiency and reducing its size, weight and power (SWAP). Besides, to enter into competition with modern DRFM, some important parameters such as time-delay interval and gradations, IBW, and so on, should be significantly enhanced. In order to overcome the issues, our group for a number of years has been studying an approach related to the development of new optimal principles and scheme to design a hybrid PRFM with the function of providing multiple replicas of a single input RF signal (Belkin, 2016;Belkinet al., 2017). Following it, we proposed the advanced concept for circuit optimization of long-term fiber-optic PRFM: distributed structure of low-power emitters based on dense wavelength division multiplexing (DWDM), multicore optical fiber (MCOF) as retarding medium, two-stage processing including optoelectronic repeater unit, and simpler RDL-based time-delay circuit using a small number of round trips so as to ensure minimal SNR degradation. In progress of that proof-of-concept study, below we demonstrate the modeling results that validated multiplication effect, as well as the device schematic and prototyping results that confirmed the quality and advantage of the PRFM under investigation. The remainder of the paper is organized as follows. Section II describes basic block diagram of PRFM to be proposed and specific schematic diagram of the prototype's MWP backbone. In addition, a brief theory confirming existence of RF signal multiplication effect is attached. Section III highlights structural peculiarities and key characteristics of the 7-core fiber delay lines that are included in the prototype. Section IV presents the test results of the prototype key characteristics as compared to available BiFODLs. In Section V, we fulfil functional, design, and parametric comparison of the PRFM has been developed, available PRFMs (Koffman,1988;Nguyen, 2014) and DRFMs of last generation. Section VI concludes the paper.

II. PROPOSED PRFM DESCRIPTION

Figure 1 shows the PRFM basic block diagram including the principal units of microwave photonic backbone: Optical Generation and Modulation Unit (OGMU), Initial Optical Processing Unit (IOPU), Optoelectronic Re-transmission Unit (OERTU), and Final Optical Processing Unit (FOPU). One can realize their functionalities from the titles. Each of the elements is controlled by Electrical Control Unit that contains AC/DC power converters, modules for temperature and power stabilization of the lasers' operating modes, modules to control and status monitoring optical switches and attenuators. Besides, the PRFM block diagram includes 32-position Push Button Module for the arrangement on the front panel.

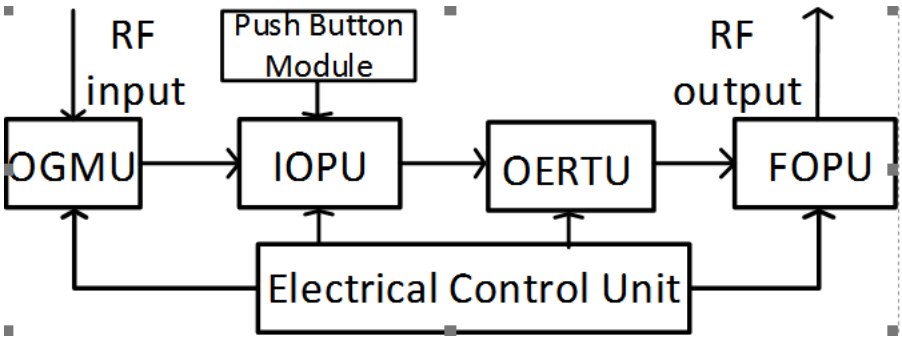

Figure 1: Basic block diagram of the developed PRFM.

Figure 2 depicts in detail the schematic diagram of the prototype MWP backbone. Following the first proposed principle (Belkin,2016) OGM unit contains eight low-power distributed feedback lasers emitting in the channels 53-60 of 100GHz-DWDM grid coinciding with ITU-T Recommendation G.692. Although, another set of C- or L-band optical channels is feasible too. To cancel chirping effect of the direct modulation, Optilab DFB-1550-EAM-12 laser diodes with integrated electro-absorption modulator (EAM) supporting 12-GHz external modulation bandwidth were utilized in the prototype. Refusal of lithium-niobate electro-optic MZM used as standard in FODLs (Urick et al., 2015) allowed us to reduce remarkably insertion loss, which requires a strong-power laser as an input, and to gain the cost. The same modulation signal inputs to all laser diodes through RF splitter.

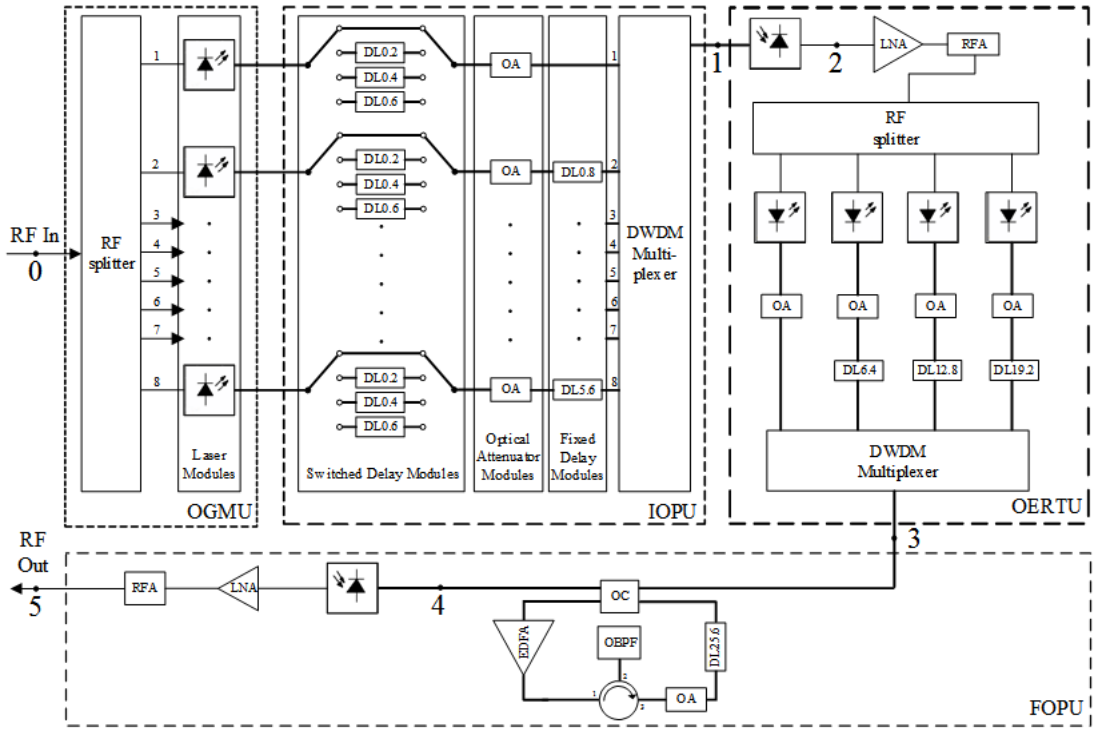

Figure 2: Schematic diagram of the prototype's MWP backbone. DL – Delay Line (The digits indicate the delay time in microseconds), OA – Optical Attenuator, LNA – Low Noise RF Amplifier, RFA – Radio Frequency Attenuator, OC – Optical Coupler, EDFA – Erbium Doped Fiber Amplifier, OBPF – Optical Band Pass Filter. Thick line means optical connection, thin line means RF connection.

IOP unit fulfils the operation of switchable and fixed delays for each optical channel after that combining them through DWDM spectral multiplexer. The unit includes eight segments of switchable FODLs for a delay of 0-0.6 μs with 0.2-μs increment and eight segments of fixed FODLs for a delay of 0-5.6μs with 0.8-μs increment. Using in the prototype 7-core MCOF allowed us to accommodate as many as 31 delay lines in a single reel of rather small dimensions. In turn, application of OERT unit summarizes all delay gradations of the IOPU taking advantage of a wide spectral passband of InGaAs pin-photodiode. The photo-detected RF signal is amplified, divided into 4 ways, and modulates four laser diodes of the same model as in OGMU emitting in the channels 26-29 of 100GHz-DWDM grid. Also, any other C-band and even the same optical channels as in OGMU are feasible. Then, each of four optical channels undergoes delays of 0.0, 6.4, 12.8 or 19.2μs, respectively, which are realized by the single 7-core MCOF too. After that, all channels are combined in the second DWDM multiplexer. Terminating the MWP backbone, FOP unit realizes the last design principle (Belkin,2016) using an optical RDL with the delay of 25.6 μs in its feedback circuit. Finally, all delayed replicas are converted again in RF band. After that, they are amplified and output. Notice that the powers of all optical signals in IOPU and FOPU are adjusted correspondingly by optical attenuators (OA), which are regulated through the Electrical Control Unit.

Initial computer-aided simulation was fulfilled elsewhere (Belkin et al., 2017) so below we present some calculation results of the proposed PRFM operation using ideal models of the circuit elements to demonstrate effect of replica multiplication. Suppose that its input (point 0 of Fig. 2) is fed by a periodic sequence of Gaussian RF pulses with a period greater than the maximum provided delay. The dependence from time t results in:

$$SR(0) = U_0 \cdot \exp\left(-\frac{t^2}{\sigma^2}\right) \cdot \sin(\Omega t), \qquad (1)$$

where $U_0$is the amplitude of the input RF signal, Ω is angular frequency of the RF carrier, and σ is the time constant associated with the full width at half maximum (FWHM) τ_s of the pulse as $\sigma = \tau_s/2\sqrt{\log_e 2}$. Then, wavelength-multiplexed optical signal at the output of IOPU (point 1 of Fig. 2) after intensity modulation and initial delay is in time domain:

$$SO(1) = \sum_{n=1}^{8} (A_0 + M_n \cdot \exp\left(-\frac{\tau_n^2}{\sigma^2}\right) \cdot \sin(\Omega\tau_n)) \cdot k_n \cdot s_n \cdot \sin(\omega_n \cdot \tau_n), \qquad (2)$$

where A_0 is the value of DC bias of the EAM's light-voltage characteristic (near the center of the linear area), $M_n$is intensity modulation depth of n-th optical carrier (M_n<1), $\tau_n = t - \tau_{d,n}$, where $\tau_{d,n}$ is time delay in n-th optical channel; k_n is gain factor of n-th optical channel, S_n and ω_n are amplitude and angular frequency of the n-th optical carrier, correspondingly, and n is the number of optical channel in IOPU. After O/E conversion the RF waveform at the output of the first photodetector (point 2 of Fig. 2) will be:

$$SR(2) = \sum_{n=1}^{8} U_n \cdot \exp\left(-\frac{\tau_n^2}{\sigma^2}\right) \cdot \sin(\Omega\tau_n), \quad (3)$$

where U_n is the photo-voltage amplitude under the power of n-th optical channel; $U_n = 0.5R_1 \cdot (A_n \cdot M_n \cdot k_n)^2 \cdot r_l$, where R_1 is the responsivity (A/W) of the first photodetector, A_n is the level of n-th optical carrier, r_l is the load resistance. Optical signal at the output of the prototype's OERTU (point 3 of Fig. 2) after the second E/O conversion, second procedure of time delay, and subsequent wavelength multiplexing is represented by:

$$SO(3) = \sum_{m=1}^{4}\sum_{n=1}^{8}(A_0 + M_{nm} \cdot \exp\left(-\frac{\tau_{nm}^2}{\sigma^2}\right) \cdot \sin(\Omega\tau_{nm})) \cdot k_m \cdot s_m \cdot \sin(\omega_m \cdot \tau_m), \quad (4)$$

where M_{nm} is the M_n-dependent resulting intensity modulation depth of m-th optical carrier (M_m<1), $\tau_{nm}= t - \tau_{d,n} - \tau_{d,m}$, where $\tau_{d,m}$is time delay in m-th optical channel of OERTU; k_m is gain factor of m-th optical channel, S_m and ω_m are amplitude and angular frequency of the m-th optical carrier, correspondingly, and m is the number of optical channel in OERTU.

It follows from Fig. 2 that the key element of FOPU is optical recirculation loop with active feedback for the loss compensation. Equation (4) represents its output optical signal (point 4 of Fig. 2) taking into account the first three round trips.

$$SO(4) = p \cdot \sum_{i=0}^{3}\sum_{m=1}^{4}\sum_{n=1}^{8}(A_0 + M_{nm} \cdot \exp\left(-\frac{\tau_{nmi}^2}{\sigma^2}\right)\sin(\Omega\tau_{nmi})) \cdot k_{mi} \cdot s_m \cdot \sin(\omega_m \cdot \tau_{mi}) \cdot (1-p)^i, \quad (5)$$

where p is insertion loss of X-type optical coupler between points 3 and 4, $\tau_{nmi}=\tau_{nm}-i.\tau_{dlC}$, $\tau_{mi} = \tau_m - i.\tau_{dlC}$. Here, τ_{dlC} is overall time delay in recirculating loop during one round trip; $k_{mi} = k_m \cdot k_{OA}^i \cdot k_C^i$, where k_{OA} is gain factor of the EDFA, k_C is round-trip loss in the recirculating loop, $k_C \leq 1$, and i is the number of round trip. Finally, Equation (6) represents PRFM output signal (point 5 of Fig. 2) after photodetector and RF amplifier.

$$SO(5) = p \cdot \sum_{i=0}^{3}\sum_{m=1}^{4}\sum_{n=1}^{8} U_{nmi} \cdot \exp\left(-\frac{\tau_{nmi}^2}{\sigma^2}\right) \cdot \sin(\Omega\tau_{nmi})) \cdot (1-p)^i, \quad (6)$$

In this expression, $U_{nmi} = r_l \cdot R_2 \cdot (S_m \cdot M_{nm} \cdot k_{mi})^2$ is the amplitude of RF signal, where R_2 is the responsivity of the second photodetector. The remaining notation is the same as before.

Figure 3 shows some MathCAD calculation results referred to interim point 2 (a), and output point 5 for the cases of direct trip (b) and one round-trip (c) in the optical recirculation loop. For better vision we used only four optical channels in IOP unit (n=1, 3, 5, 7).

The numerous replicas of a single input RF signal depicted in this Figure clearly confirm the correctness of our approach.

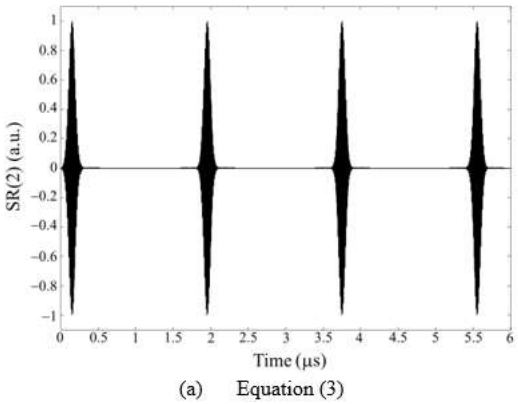

(a) Equation (3)

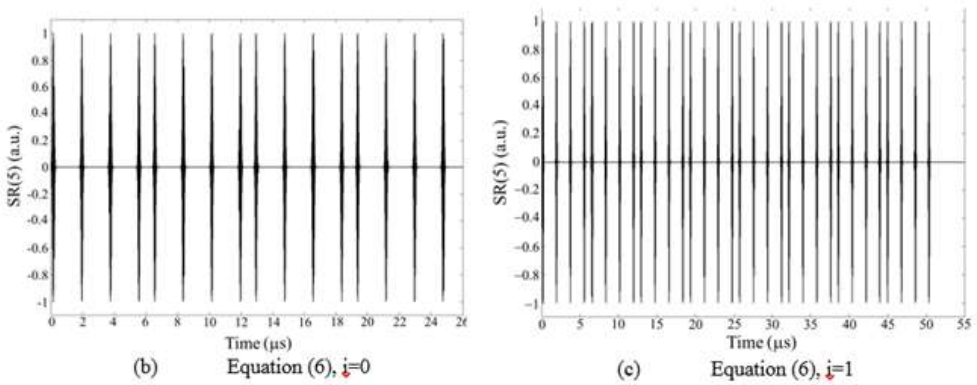

Figure 3: MathCAD calculation results.

III. MULTICORE DELAY LINES

As one can see from Fig. 2, there are three units in the prototype including fiber-optic delay lines of the length in the range from near 40 m to more than 5 km. Using multicore fibers, which are now widely investigated in telecommunication area (Zhu et al., 2010; Machoet al., 2016), permitted us to make these FODLs more compact that is particular important if long time delays are required (Egorova et al., 2017). To interconnect efficiently with standard single-mode optical fiber, each delay module consists of multi-core fiber of required length and fan-in/fan-out devices, which extract optical signals from one core of multicore fiber to individual single-core fiber. Multicore fibers used in the PRFM prototype have seven cores of a hexagonal configuration in the cross section. Core diameters were approximately 9.0 μm, core-cladding refractive index difference 0.0055, measured cutoff wavelengths for all cores were in the range of 1.47 – 1.48 μm. Distance between centers of neighboring cores was 44.5 μm, diameter of silica cladding was 205 μm. For realization of fan-in /fan-out devices, we used the method based on etching and gluing of the single core fibers (Watanabe K.et al., 2012). The details of fabrication and standard characterization for the 7-core FODLs are described in our previous papers (Egorova et al., 2017;Egorova et al., 2016).

The main feature of the use of multi-core fiber in delay lines is the need to transfer optical signals with analog modulation. In this regard, specific parameters are becoming important that are not given sufficient attention in digital fiber-optic systems, such as loss, reflections, crosstalk, group time delay (GTD) stability, dynamic range, etc. First, we focused on studying the propagation features for our FODLs based on 7-core MCOF. Table 1 lists the typical results of testing overall insertion loss including fiber core and two terminal fan-outs, reflections from fan-out, and crosstalk levels between the cores. The measurements were carried out on a sample of a 160-m MCOF used in the switchable delay module of the IOPU. As one can see from the Table, all the MCOF-under-test parameters, especially reflections from a fan-out are feasible for practical purposes. Notably, total optical losses in each channel were not greater than 2 dB, reflections were less than -46 dB. In addition, the crosstalk was lower than -51 dB. It should be note that the optical loss at side cores joints of first fan-out is higher than at the central cores joint of first fan-out and at all joints of second fan-out. The reason is that during the installation process the distance between centers of neighboring cores in the first fan-out was not well coincide with core-to-core distance in the fiber. Due to core-to-core distance mismatch between fiber and first fan-out, side cores have transverse offset at joins leading to increased optical losses.

Table 1. Typical Parameters of Delay Module Based on 7-Core Fiber

Core nember	First fiber/fanout joint (dB)		Second fiber/fanout joint (dB)		Total Losses (dB)	Crosstalk Between central and side channels (dB)
	Optical losses (dB)	Reflection (dB)	Optical losses (dB)	Reflection (dB)		
0 (central)	0.6	-51.6	0.3	-53	1.0	-
1	0.9	-64	0.4	-62.7	1.4	-55.6
2	1.5	-46.1	0.4	-47.9	2.0	-53.7
3	1.6	-50.7	0.3	-49.9	2.0	-51.7
4	0.9	-46.1	0.6	-50.8	1.6	-52.1
5	1.0	-58.5	0.4	-56.3	1.5	-54.1
6	1.1	-46.8	0.5	-57.3	1.7	-53.4

Application of a 7-core fiber instead of a single-core one enables in principle a seven-fold reduction in the total fiber length necessary for obtaining a required time delay that results in shortening overall sizes of the device. On the other hand, it is well known (Zhu et al., 2010) that bending the fiber in the process of winding onto the spool can lead to some parametric degradation, for example, to a difference in GTD of the central and

side cores. Consequently, in the course of multicore FODL prototyping, an issue associated with estimating the minimum allowable winding radius, which limits the possibility of reducing its sizes, was arisen. This fact was taken into account when designing FODL for the PRFM prototype (Egorovaet al.,2016) and we believe that bending loss of our fiber is not higher than for standard telecom fibers referred to G.652.

Figure 4 shows IOPU's delay module including 31 fiber-optic delay lines based on 7-core single-mode fiber (8 FODL of 0.2 μs, 8 FODL of 0.4 μs, 8 FODL of 0.6 μs, 1 FODL of 0.8 μs, 1 FODL of 1.6 μs, 1 FODL of 2.4 μs, 1 FODL of 3.2 μs, 1 FODL of 4.0 μs, 1 FODL of 4.8 μs, 1 FODL of 5.6 μs).

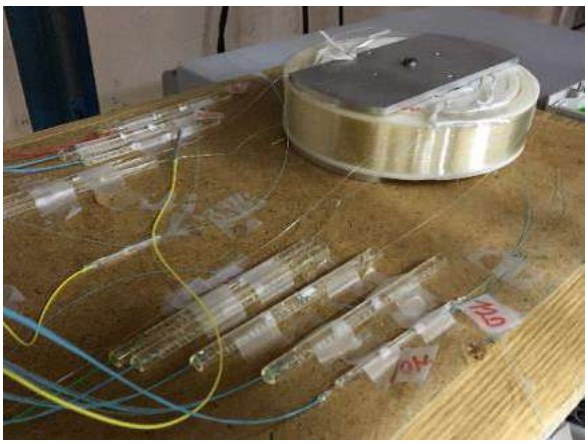

Figure 4: IOPU's delay module containing 7-core single mode fiber reel (diam. 150 mm, height 30 mm) and fan-outs (located on the left side of the reel).

IV. PRFM PROTOTYPE INSPECTION AND CHARACTERIZATION

The proof-of-concept experiments for PRFM to be proposed were described elsewhere (Belkin,2016). This time, we present the prototyping and measurement results of the prototype key characteristics as compared to the available FODLs.

Figure 5 depicts Optical Generation and Modulation Unit (a) assembled in accordance with Schematic diagram of Fig. 2, and measured spectral characteristics on its output (b). The unit is a compact three-tiered structure containing four laser modules on the first and third stages and a 1-to-8 RF splitter on the intermediate stage. As follows from Fig. 5(a), each laser module includes Optilab DFB-1550-EAM-12 laser diode (1) and homemade card for its temperature and power stabilization (2). Input (3) and interconnect (4) RF coaxial cables are also shown in this Figure.

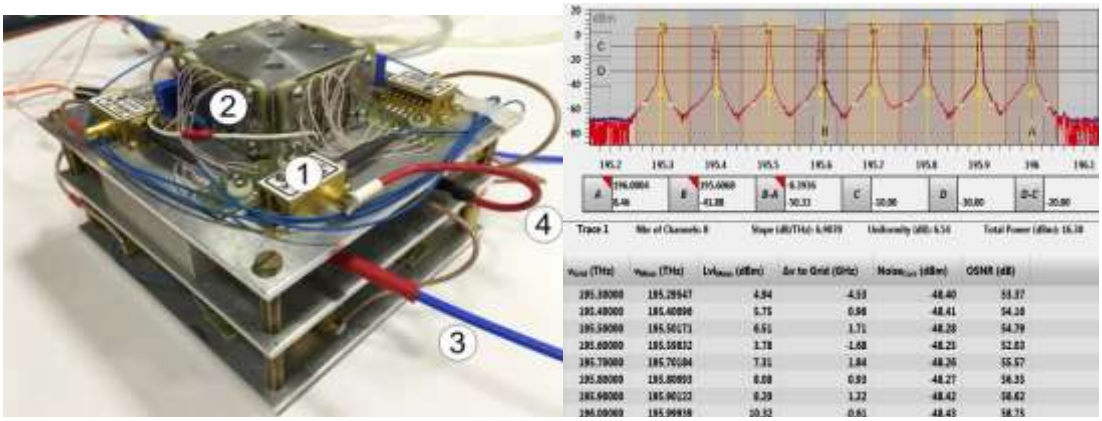

(a) (b)

Figure 5: Assembly of Optical Generation and Modulation Unit (a), and output optical spectrum (b).

It follows from Fig. 5 (b), all laser modules have approximately the same power with a deviation in the range of 3 dB, and their emission frequencies are practically at the center of the channels 53-60 for 100GHz-DWDM grid with a deviation of no more than 4 GHz. In addition, high-quality optical signals are provided with an optical power-to-noise ratio (OSNR) of more than 50 dB.

Figure 6 depicts Optoelectronic Re-Transmission Unit (a) assembled in accordance with Schematic diagram of Fig. 2, and converted to RF band signal oscillogram (b) on its output. The unit consists of Gooch&Housego EM169 photodetector (1) with the bandwidth of 20 GHz, low-noise (2) and power (3) RF

amplifiers, compact two-tiered structure (4) containing the same as in OGMU four laser modules on the lower stage and a 1-to-4 RF splitter (6) on the upper stage, and fixed RF attenuator (5).

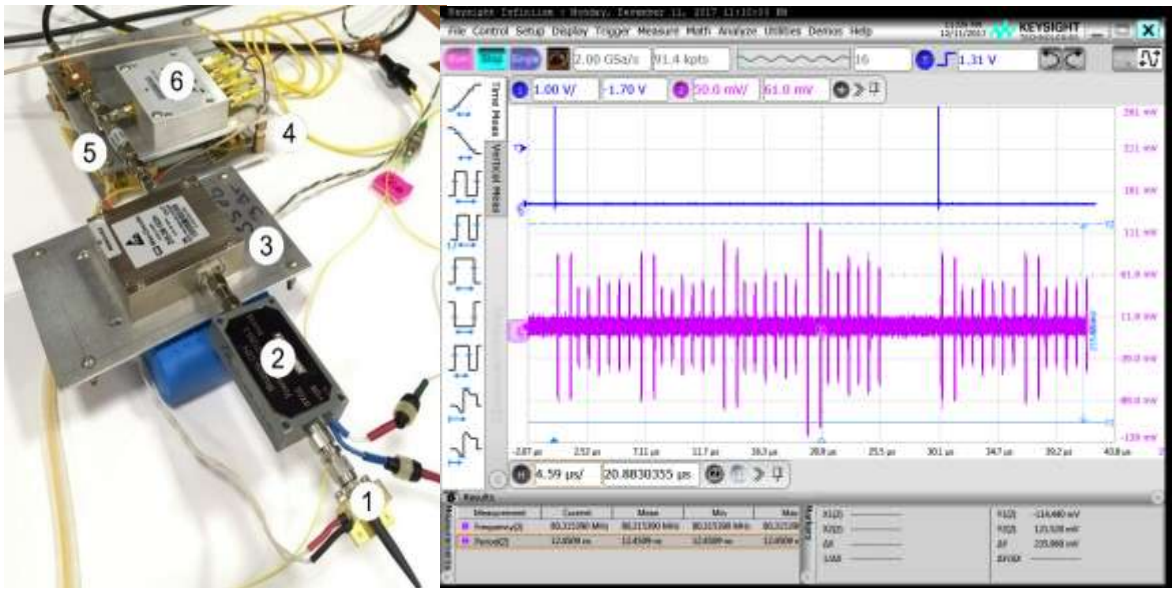

(a) (b)

Figure 6: Assembly of Optoelectronic re-transmission unit (a) and oscilloscope pattern (b)of RF pulses at the output (point 3 of Fig. 2). Vertical scale is 50 mV

It follows from Fig. 6 (b), oscillogram in RF domain verifies signal multiplication effect that was predicted by the theory in Section 2. There are two traces in the Figure: the upper one depicts a period of input RF pulse sequence (RF carrier 10 GHz, pulse width 0.1 μs, period 30 μs); the lower one shows 32 RF pulses formed in IOP and OERT units. Note that herein and after in Fig. 7(b) and Fig. 8(b) the substantial non-uniformity of the amplitudes of the pulses (up to 2 times) in the plots is a consequence of the absence of optical attenuators with suitable attenuation for the all optical channels at the time of measurements. However, the reproduction effect is clearly visible.

Figure 7 depicts Optical Recirculation Loop (a) assembled in accordance with Schematic diagram of Fig. 2, and measured down-converted to RF band signal oscillogram on its output (b). The unit consists of optical X-coupler (1), Erbium doped fiber amplifier with a driver (2), optical band pass filter (3) connected through a circulator (4), optical attenuator (5), and FODL (6) of 25.6 μs. To avoid too much loss in the loop, the last element is realized based on a standard single-mode fiber. Fig. 7(b) demonstrates output sequence of three RF pulses containing a primary pulse train that has tripped without delay (left), and its three delayed replicas, sequentially passing through the recirculation loop. Following the Figure, the quality of RF output waveforms even after three round-trips is sufficient for further processing.

The general layout of the PRFM prototype's MWP backbone and the oscillogram of the output signal (point 5 of Fig. 2) including 96 RF pulse simultaneously, are shown in Fig. 8.

As known (Urick et al., 2015) the key parameter of any MWP apparatus is Spurious Free Dynamic Range (SFDR). The third-order SFDR usually studied for MWP-based radio-electronic systems is determined by calculation using some measurement data, such as noise power spectral density and third-order output intercept point (OIP3), which, in turn, is the power difference in dBm at the fundamental and third harmonics of the output signal (Urick et al., 2015). When substituting the measured data in the formulas of (Urick et al., 2015), the third-order SFDR = 90 dB•$Hz^{2/3}$.

Finally, Table 2 lists the results of the PRFM prototype characterization as compared to state-of-the-art FODL (Urick et al., 2015;Diehlet al., 2015). As one can see, the developed device has significantly better parameters, except for the upper operating frequency, which is exclusively determined in the Prototype by the modulation bandwidth of the applied laser module. In particular, the adopted design principles allowed to ensure a sufficiently deep memorization of the input signal, to increase the number of reproduced delay gradations, and to reduce the occupied volume by more than 3 times.

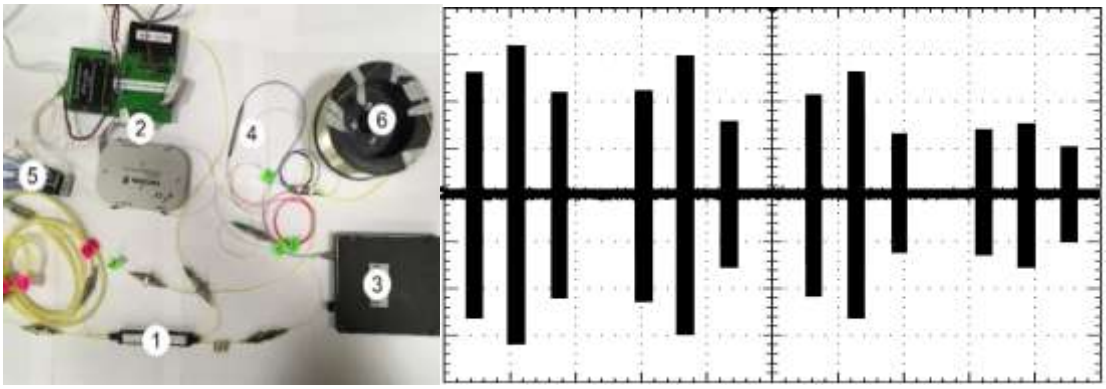

(a) (b)

Figure7. Assembly of Optical Recirculation Loop (a) and oscillogram (b) of down-converted to RF band pulses at the output (point 4 of Fig. 2).

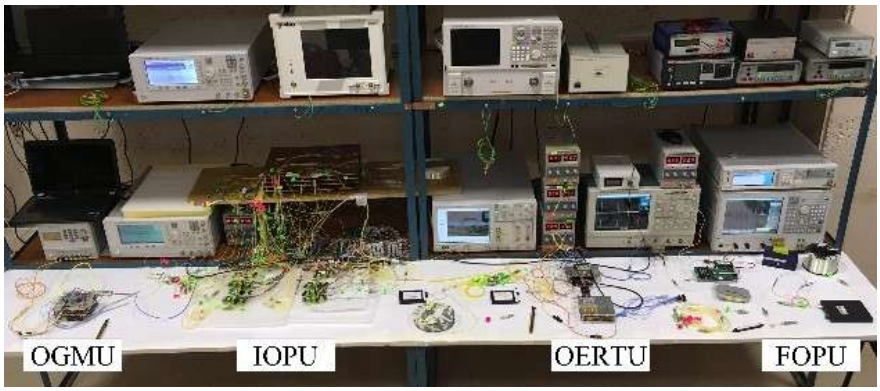

(a)

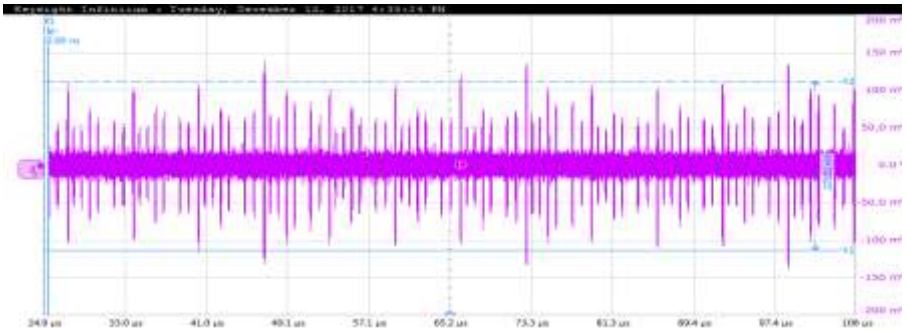

(b)

Figure8. PRFM prototype on the table of test bench (a) and the oscillogram of its output RF signal (b).

Table 2. Comparison with State-Of-The-Art Fiber-Optic Binary Delay Line

Parameter	State-of-the-FODL[4,6]	This prototype
Operating frequency range (GHz)	0.5-18	0.1-12
Number of simultaneous signal replicas at the output	1	128
Number of reproduced delay gradations	512	More than 1M
Step of time gradation (μs)	1	0.2
Dynamic range ($dB \cdot Hz^{2/3}$)	88	90
Sizes (mm)	648x432x222	425x365x125

V. COMPARISON WITH AVAILABLE PRFM AND DRFM

In order to determine clearly the pros and cons of the proposed multi-stage PRFM, its suitability for radar test and evaluation, anti-radar ECM techniques, or another civil and military MWP equipment, and to identify tasks and ways to further improve the proposed technique, below, some functional, designing, and parametric features of proposed and already known PRFMs or modern DRFMs are compared.

It follows from Introduction that all known PRFMs have been designed exclusively on the basis of simple optoelectronic (Koffman et al., 1988) or all-optical (Nguyenet al., 2014) recirculating loop. Due to this fact, their parameters do not meet the modern requirements of practical radars and ECM means. To clear it, Table 3 lists parametric comparison of the available approaches and the above-described PRFM prototype.

Table 3. Comparison of the Known PRFM Design Examples vs. the Developed PRFM Prototype

PARAMETER	(Koffman et al.)	(Nguyen et al.)	THIS PAPER	PROS AND CONS
RF operating range (GHz)	2-6	<0.5	0.1-12	Much wider; almos meets the requirements for modern radars
Needed recirculation number	28	200	3	Noise reduction in a simple and cost-efficient RDL structure
MAX. RF pulse duration (μs)	Up to 0.2	Up to 1.5	Up to 25	Meets the requirements for modern radars
Time delay interval (μs)	0.2	1.5	0.2-77	Meets the requirementsfor modern radars
Number of simultaneous replicas at the output	1	1	Up to 128	Improves the accuracy of determining the location of the object
Number of stage	1	1	4	-

As one can see from the Table, the capabilities and parameters of the proposed approach significantly exceed the known functional analogs at the expense of schematic complexity.

Generally, current state-of-the-art DRFM systems are challenged functionally by the advanced emitters due to limited instantaneous bandwidth and sensitivity; incident waveform dependent; distortion of target's fidelity in the process of phase quantization; limited number of overlapping targets; high latency that decays the self-defense capability. Table 4 lists some design and parametric features of proposed PRFM and a forecast for 5-th generation DRFM (Olivier, 2011).As one can see from the Table, the capabilities and parameters of the both approaches are comparable with each other. However, DRFM has a number of specific drawbacks, in particular, the need for additional conversion to digital form, relatively high power consumption, operation in a limited frequency range, which in most practical cases requires an additional up and down frequency conversions, higher latency, and the need for careful shielding of analog and digital circuits.

Table 4. Comparison of the Fifth Generation DRFM Modules vs. the Developed PRFM Prototype

Feature/Parameter	DRFM	Proposed PRFM	Comment
Formats of radio signals	Pulse and continuous	Pulse and continuous	In accordance
Multiple delayed replicas	Yes	Yes	In accordance
Typical circuit structure	Down/up frequency conversion, analog-to-digital delay, digital signal processor	Modulation and detection in optical range, fiber-optic delay lines on MCOF	Much easier (potential gain in size, weight and power)
Functionality	Multifunctional, capable to work in various modes of radar suppression, and form numerous false images of goals	Capable to form rather simple false images of goals controlling by optical attenuators	Worse. Further research is require
Time delay inteval	20 ns-2s	0.2-77 μs	Worse. Further research is required
Memory depth	200 ms	Real time processing	Better
Latency (ns)	Up to 50ns	Near 50ns	Better
Operating frequency range (GHz)	0.1-2 (for higher frequencies, down and up frequency converters are required)	0.1-12 (without PF frequency converters)	Better
Instantaneous bandwidth (MHz)	100-2000	Almost 12000	Better
Dynamic range (SFDR, dB)	60	90	Much better
Size/Weight	200x65x50 mm/0.5kg (without	425x365x125 mm/8kg	Worse. Further research is required

	frequency converters)		

VI. CONCLUSION

A novel Photonic radio-frequency memory based on microwave photonics and multicore fiber techniques is proposed and a test prototype is fabricated and investigated. The main building blocks of proposed memory are (i) an assembly of low-power emitters for dense wavelength division multiplexing, (ii) multicore optical fiber as retarding medium, (iii) two-stage processing, (iv) optoelectronic re-transmitting unit, and (v) optical recirculation time-delay circuit. The memory features of the prototype were compared with the performances of widespread binary fiber-optic delay lines. A sufficiently deep memorization of the input RF signal and increased number of reproduced delay gradations were demonstrated in a reduced volume of the assembly. The results of the prototype examination as compared to the known versions of Photonic radio-frequency memory showed that the adopted design concept allowed to ensure a sufficiently deep memorization of the input RF signal, to increase the number of reproduced delay gradations, and to successfully process all the radar's radio frequency pulse width, which extends from several hundred of nanoseconds to tens of microseconds, in a multi-octave RF operating range. As demonstrated through functional and parametric comparison of the Photonic radio frequency memory approach has been developed, and last-generation Digital radio-frequency memory, which has being modernized for 20 years; their capabilities and parameters are comparable. However, the latter has a number of specific drawbacks, in particular, the need for additional conversion to digital form, relatively high power consumption, operation in a limited frequency range, which in most practical cases requires additional up and down RF conversions, the need for careful shielding of analog and digital circuits.

The challenges of increasing the proposed memory performances are discussed and a roadmap of next steps is proposed as well.

REFERENCES

[1]. Baldwinson J. andAntipov I., "A modelling and simulation tool for the prediction of electronic attack effectiveness," in Proceedings of Association of Old Crows Int. Symp., Adelaide, Australia (2008).

[2]. Belkin M. E.; Bakhvalova T. N.;Gladyshev I. V.;Egorova O. N.; Semenov S. L., "Continuously accessible long-term fiber optic memory of microwave signal," in 2017 International Topical Meeting on Microwave Photonics (MWP), 1-3 (2017), Beijing, China.

[3]. Belkin M.E., "Design principles of long-term analog RF memory based on fiber-optics and microwave photonics approaches", in Proceedings of IEEE Avionics and Vehicle Fiber-Optics and Photonics Conference (AVFOP), 21-22, California USA (2016).

[4]. Capmany J. and Novak D., "Microwave photonics combines two worlds," Nat. Photonics **1**, 319-330 (2007).

[5]. Diehl J. F., Singley J. M., Sunderman C. E., and Urick V. J., "Microwave photonic delay line signal processing," Appl. Opt. **54**(31), F35-F41 (2015).

[6]. Egorova O.N., Astapovich M.S., Belkin M.E., Semenov S.L., "Fiber-Optic Delay Line using Multicore Fiber," Bull. Lebedev Phys. Inst. **44**(1), 5-7 (2017).

[7]. Egorova O.N., Astapovich M.S.,Belkin M.E.,Semjonov S.L., "Multicore optical fibre and fibre-optic delay line based on it," Quant. Electronics **46**(12), 1134 – 1138 (2016).

[8]. http://ieeexplore.ieee.org/xpl/conhome.jsp?punumber=1000458

[9]. Koffman I., Herczfeld P. R.,Daryoush A. S., B. Even-Or, and R. Markowitz, "A fiber optic recirculating memory loop for radar applications," Microw. Opt. Technol. Lett. **1**(7), 232–235 (1988).

[10]. Kwak C. M., "Application of DRFM in ECM for pulse type radar," presented atthe 34th International Conference on Infrared, Millimeter, and Terahertz Waves, 1-2 (2009).

[11]. Macho, Morant M., and Llorente R., "Next-Generation Optical Fronthaul Systems Using Multicore Fiber Media," IEEE J. of Lightwave Technol. **34**(20), 4819-4827 (2016).

[12]. Nguyen T. A.,Chan E. H. W., andMinasian R. A., "Photonic Radio Frequency Memory Using Frequency Shifting Recirculating Delay Line Structure," IEEE J. of Lightwave Technol. **32**(1), 99-106 (2014).

[13]. Olivier K. andGouws M., "Modern Wideband DRFM Architecture and Real-time DSP Capabilities for Radar Test and Evaluation," presented at Saudi International Electronics, Communications and Photonics Conference, 1-4 (2013).

[14]. Olivier K., "Advances in DRFM technology during the past decade and its importance as part of EW suit," Aardvark Roost AOC Conference, CSIR, Pretoria, South Africa, Sept. 2011.

[15]. Seeds J.,Williams K.J., "Microwave Photonics," IEEE J. of Lightwave Technol. **24**(12), 4628-4641 (2006).

[16]. Urick V. J., McKinney J. D., and McKinney K. J. x, Fundamentals of microwave photonics, (John Wiley & Sons, 2015).

[17]. Watanabe K., Saito T.,Imamura K.,Shiino M., "Development of Fiber Bundle Type Fan-out for Multicore Fiber," in the 17th Opto-Electronics and Communications Conference (OECC 2012) Technical Digest, July 2012, Busan, Korea, Paper 5C1-2, 475-476 (2012).

[18]. Yao J., "Microwave Photonics," IEEE J. of Lightwave Technol. **27**(3), 314-335 (2009).

[19]. Zhu B., Taunay T. F.,Yan M. F.,Fini J. M.,Fishteyn M.,Monberg E. M., andDimarcello F. V., "Seven-core multicore fiber transmissions for passive optical network," Opt. Express **18**(11), 11117-11122 (2010).

Mikhail E. Belkin" Reproducing Photonic Radio-Frequency Memory Based on Multicore Fibers" International Journal Of Engineering Research And Development , vol. 15, no. 3, 2019, pp 59-68